Depolarization Parameter in Proton-Proton Scattering at 213 MeV*

KAZUO GOTOW, FREDERICK LOBKOWICZ, AND ERNST HEER†
Department of Physics and Astronomy, University of Rochester, Rochester, New York
(Received April 20, 1962)

The depolarization parameter, D, in p-p scattering at 213 MeV has been measured over the angular range 30–90° c.m. The results have been included in the modified phase-shift analyses performed by MacGregor *et al.* and by Signell, which have yielded a unique phase-shift set for p-p interaction at this energy. The results of the experiment are also compared with the predictions by the semiphenomenological potentials of Bryan and of Hamada.

I. INTRODUCTION

IN the past several years there has been a great deal of effort to make a complete determination of the nucleon-nucleon scattering matrix at several interaction energies between 95 and 310 MeV[1] by use of polarized nucleon beams.[2] This paper is a continuation of the work on a proton-proton scattering program[3] which has been in progress at the Rochester Synchrocyclotron Laboratory to obtain a unique set of p-p scattering phase shifts at a laboratory kinetic energy of 213 MeV.

The R and A parameters[3] measured at seven angles between 30 and 90° in the center-of-mass system, together with previously obtained p-p scattering asymmetry[4] and cross section,[5] have already yielded four acceptable phase-shift solutions for 213 MeV[6] (labeled by a, b, c, and d). It has been noted that solutions a and c do not correspond to either of the two acceptable phase-shift solutions at 310 MeV.[7] Our preliminary data of the depolarization parameter D at 30 and 60° c.m.[8] agreed with the values predicted by either solution b or c, while solutions a and d predicted quite different values.

A later search of the phase shifts,[9] which included the preliminary result for the D parameter, indicated a strong preference for solution type b over solution type c, while the others were ruled out.

In this report we present the result of depolarization measurements at 213 MeV for 30, 40, 50, 60, 70, 80, and 90° c.m.

The general expression for the polarization $\mathbf{P}_f$ produced by the scattering of incident protons with polarization $\mathbf{P}_i$ off unpolarized protons is

$$\mathbf{P}_f=(1+P_2\mathbf{P}_i\cdot\mathbf{n}_2)^{-1}\{(P_2'+D\mathbf{P}_i\cdot\mathbf{n}_2)\mathbf{n}_2 +[A\mathbf{P}_i\cdot\mathbf{k}_2+R\mathbf{P}_i\cdot(\mathbf{n}_2\times\mathbf{k}_2)](\mathbf{n}_2\times\mathbf{k}_2') +[A'\mathbf{P}_i\cdot\mathbf{k}_2+R'\mathbf{P}_i\cdot(\mathbf{n}_2\times\mathbf{k}_2)]\mathbf{k}_2'\}, \quad (1)$$

where $\mathbf{k}_2$ and $\mathbf{k}_2'$ are the unit vectors along the momentum of the incident and scattered protons, $\mathbf{n}_2$ is the unit vector normal (in the direction $\mathbf{k}_2\times\mathbf{k}_2'$) to the scattering plane, and P_2, P_2', D, A, R, A', and R' are the scattering parameters.

We use the nomenclature introduced by Wolfenstein[10] with the modification that we discriminate between P_2', the polarization produced by unpolarized p-p scattering, and P_2, the asymmetry produced at the hydrogen scattering by a completely polarized incident proton beam.

One has to perform a third scattering to measure $\mathbf{P}_f$. The left-right asymmetry e in the analyzing scattering is given as follows:

$$e=(L-R)/(L+R)=P_3\mathbf{P}_f\cdot\mathbf{n}_3, \quad (2)$$

where P_3 is the analyzing power of the scattering, and $\mathbf{n}_3$ is the unit vector normal to the third-scattering plane, and L and R designate the counting rates for the left and right third scattering. For the measurement of the depolarization parameter D, all scatterings are coplanar. The external proton beam is polarized by scattering the internal beam of the cyclotron from a carbon target through an angle of 14.7°. This initial polarization $\mathbf{P}_i$ is perpendicular to the plane of the first scattering and is pointing "up." The vertical polarization of protons scattered right and left by a hydrogen

* Work done under the auspices of the U. S. Atomic Energy Commission.
† Now at Ecole de Physique, l'Université de Genève, Geneva, Switzerland.
[1] Proton-proton scattering experiments and its theory and analysis have been summarized in the following articles: M. H. MacGregor, M. J. Moravcsik, and H. P. Stapp, Ann. Rev. Nuclear Sci., **10**, 291 (1960); M. J. Moravcsik and H. P. Noyes, *ibid*, **11**, 95 (1961).
[2] C. L. Oxley, W. F. Cartwright, J. Rouvina, E. Baskir, D. Klein, J. Ring, and W. Skillman, Phys. Rev. **91**, 419 (1954); C. L. Oxley, W. F. Cartwright, and J. Rouvina, *ibid.* **93**, 806 (1954).
[3] A. C. England, W. A. Gibson, K. Gotow, E. Heer, and J. H. Tinlot, Phys. Rev. **124**, 561 (1961).
[4] E. Baskir, E. M. Hafner, A. Roberts, and J. H. Tinlot, Phys. Rev. **106**, 564 (1957). Recently the p-p asymmetry at this energy has been remeasured; see reference 14.
[5] C. L. Oxley and R. D. Schamberger, Phys. Rev. **85**, 416 (1952); O. A. Towler, Jr., *ibid.* **85**, 1024 (1952). The p-p differential cross section at 213 MeV has been remeasured: A. Konradi and J. H. Tinlot (private communication); also A. Konradi, Ph.D. thesis, University of Rochester, 1962 (unpublished).
[6] M. H. MacGregor and M. J. Moravcsik, Phys. Rev. Letters **4**, 524 (1960).
[7] P. Cziffra, M. H. MacGregor, M. J. Moravcsik and H. P. Stapp, Phys. Rev. **144**, 880 (1959); M. H. MacGregor, M. J. Moravcsik, and H. P. Stapp, *ibid.* **116**, 1248 (1959); H. P. Stapp, T. J. Ypsilantis, and N. Metropolis, *ibid.* **105**, 302 (1957).
[8] K. Gotow and E. Heer, Phys. Rev. Letters **5**, 111 (1960).
[9] M. H. MacGregor, M. J. Moravcsik, and H. P. Noyes (private communication). A. England, W. Gibson, K. Gotow, E. Heer, J. Tinlot and R. Warner, *Proceedings of the 1960 Annual International Conference on High-Energy Physics at Rochester* (Interscience Publishers, Inc., New York, 1960).
[10] L. Wolfensten, Ann. Rev. Nuclear Sci., **6**, 43 (1956).

target is measured with a polarimeter. The polarimeter consists of a carbon third target and a pair of triple counter telescopes. $\mathbf{n}_3$ is defined to be in the same direction as $\mathbf{P}_i$. Then, from Eqs. (1) and (2), we have the relation between P_i and the asymmetries for left or right second-scattered protons, e_L or e_R, respectively, as follows:

$$e_L(1+P_iP_2)=(DP_i+P_2')P_3, \tag{3a}$$

$$e_R(1-P_iP_2)=(DP_i-P_2')P_3. \tag{3b}$$

The experiment consists of measurements of e_L, e_R, and a calibration of the analyzing power P_3 which is performed in a properly degraded first-scattered beam by measuring the calibration asymmetry e_c:

$$e_c=P_3P_i. \tag{4}$$

II. EXPERIMENTAL ARRANGEMENT

A. Polarized Proton Beam

Production and extraction of the polarized beam was discussed in detail in a previous paper.[3] A hydrogen target was placed at $T_2(D)$, a point about 90 cm beyond the edge of the wedge magnet (see Fig. 2). The mean proton energy at the center of the hydrogen target was 213±2 MeV.[11] The energy spread in the incident beam was about 13 MeV (full width at half-maximum of the differential range curve) and the energy loss of the incident protons in the hydrogen target was approximately 8 MeV. The magnitude of the beam polarization P_i was known to be 0.89±0.02 from previous work.[12]

B. Beam Density and Energy Distributions

A detailed study was made of the horizontal beam intensity distribution and the correlation between energy and horizontal position at $T_2(D)$ and $P(D)$, a point located 188 cm downstream of the polarized beam from $T_2(D)$. The measurement was done only along the center lines of the vertical beam profiles, since the horizontal beam distributions did not change appreciably with height. A double scintillation counter telescope, whose defining crystal was a 3.2-mm cube, was used to measure integral range curves of protons at several points across the beam profiles at $T_2(D)$ and $P(D)$. We then constructed beam density distributions for various range requirements and also obtained the mean proton energy as a function of position. Figure 1 shows typical horizontal beam profiles and relations between mean proton energies and position. We

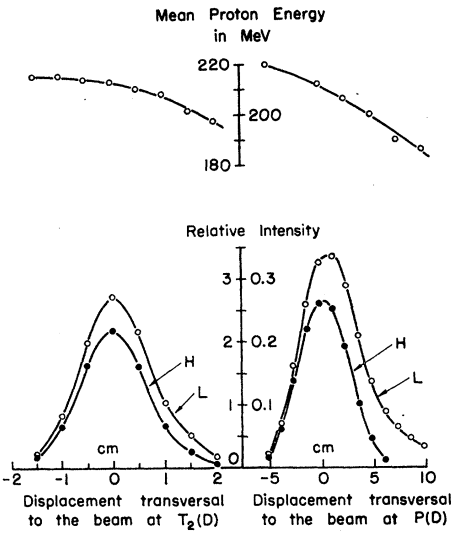

FIG. 1. Horizontal beam intensity distributions and mean-energy-position correlations at $T_2(D)$ (the left half) and at $P(D)$ (the right half). H and L indicate the high and low counting thresholds (see text) used in the beam profile measurements.

imposed several different range requirements in the asymmetry measurements for each second-scattering angle. The highest range threshold was such that we counted protons scattered from hydrogen with a mean scattering energy of more than 206 MeV. The lowest threshold corresponded to a minimum mean scattering energy of 143 MeV. The centroid of the horizontal beam distribution at $T_2(D)$ depended very little on range requirement: A shift of 1 mm was observed when range threshold was changed from the highest to the lowest.

The scanning of the beam was made at the beginning and the end of each run to check the effective beam centers at these two positions. After the run in which we collected most of the data, we found the beam line had shifted by about 30 min of arc in the second-scattering angle. Any shift of the beam line, however, did not affect the alignment of the third scattering because our alignment procedure for the analyzing scattering was made operationally, as described in III B, for each angle of the second scattering without direct knowledge of the $T_2(D)$ beam center.

C. Hydrogen Target

Liquid hydrogen was contained in a cylindrical cup 12.7 cm long by 12.7 cm in diam with a 0.13-mm thick stainless steel wall. The target was equipped with plumbing and a heater to empty the cup by remote control for background measurements. The evacuated casing of the cup consisted of a 0.76-mm thick brass cylinder with 0.05-mm thick Be-Cu windows for passing the direct beam.

The cylindrical cup was positioned with its axis vertical to the effective beam center at $T_2(D)$ when the cup was open to air. The cup was checked for its

[11] The range-energy conversion used in this article is computed from the range-energy curves of M. Rich and R. Madey, University of California Radiation Laboratory Report UCRL-2301 (unpublished) with a correction to adjust for the latest value of the mean excitation potential in copper, $I=314$ eV [R. M. Sternheimer (private communication); also see Phys. Rev. **124**, 2051(E) (1961).)

[12] W. G. Chestnut, E. M. Hafner, and A. Roberts, Phys. Rev. **104**, 449 (1956); E. M. Hafner, *ibid.* **111**, 297 (1958).

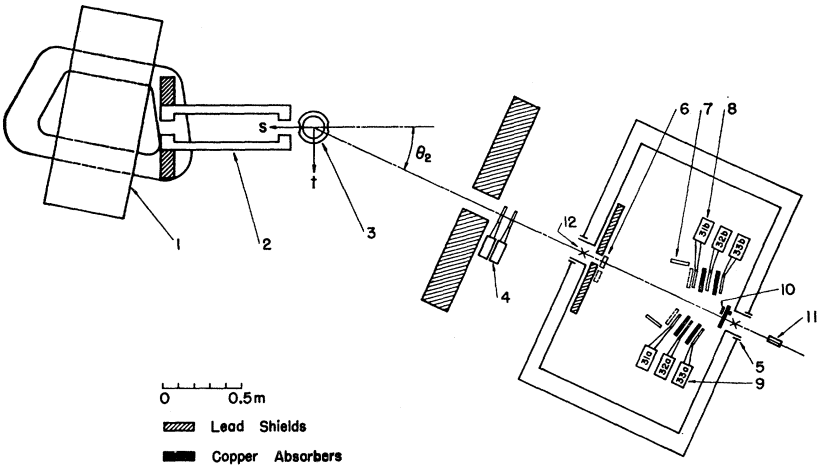

FIG. 2. Layout of the second and the third scattering. 1—Wedge magnet, 2—brass shielding, 3—hydrogen target, 4—II-telescope, 5—hollow bearing, 6—T_3, carbon target, 7—compensating absorber, 8 and 9—IIIb and IIIa telescopes, 10—B-telescope, 11—optical telescope, 12—crosshairs on the polarimeter axis.

possible movement due to evacuation and cooling by observing the displacement of the center mark on ts bottom end plate relative to the evacuated casing. The cup was thus placed at the beam center with an accuracy better than 1.6 mm in the horizontal plane. Since the size of the beam was much smaller than that of the target cup, this positioning was not critical.

D. Polarimeter

For both left and right hydrogen-scattered protons, asymmetry from the analyzing scattering was measured with the same polarimeter which was used in the previous triple-scattering measurements.

Since a detailed description of the polarimeter has been given previously,[3] we give here only a brief account of the experimental arrangement and the choices of parameters. Figure 2 shows schematically the layout of the second and the third scatterings. The slit on the polarimeter defined the beam striking the analyzing target, T_3. The telescope II, which detected the hydrogen-scattered protons, was placed as far from the slit as possible so that the protons scattered by this telescope could not reach the III telescopes. The II telescope was used also to measure range curves of the hydrogen-scattered protons for each scattering angle: it was placed in a position closer to the slit and a defining scintillation counter, which was 3.8 cm wide, 5.1 cm high, and 0.48 cm thick, was added and aligned on the rotation axis of the polarimeter. A remote-controlled absorber changer was provided, so that absorber with various thicknesses could be inserted between the two counters of the II telescope.

Two triple scintillation counter telescopes, IIIa and IIIb, in coincidence with the outputs of the II telescope were used to detect protons scattered from T_3. The dimensions of the counters and the third scattering angle were identical to those in the R and A measurements.[3] Each telescope carried copper absorbers in front of the second, 32a, or 32b, and the third, 33a or 33b, counters. Both III telescopes, including their absorbers, were made to be similar in every respect and used simultaneously in the normal and inverted position of the polarimeter.

A double scintillation telescope B was mounted on the rotating part of the polarimeter at a point 89 cm from the center of the slit. Its defining counter (0.65 cm wide, 10 cm long) was placed with its long dimension perpendicular to the polarimeter scattering plane. Profiles were measured by moving the B telescope, with proper absorber in between its two counters, horizontally along a line perpendicular to the rotation axis of the polarimeter. The telescope integrated the proton intensity over the direction of the third-scattering normal. The profile thus taken enabled us to compute the effective beam center.

The profile was measured with the polarimeter in both normal and inverted position so that one could eliminate errors originating from possible nonuniform sensitivity of the telescope along its long dimension and also could check the mechanical stability of the telescope. The profile obtained was used to align the polarimeter axis along the hydrogen-scattered beam. This will be discussed in III B.

E. Shielding

In the initial stage of the experiment a detailed study was made of the various background counting rates in order to minimize them by means of shielding. The final shielding arrangement is shown in Fig. 2; the brass shield between the wedge magnet and the hydrogen target and the lead wall in front of the polarimeter eliminated the protons scattered by air, which could trigger coincidences between the II telescope and III telescope by small angle scattering or direct penetration of T_3. At small scattering angles the direct proton beam was stopped by the lead shielding. The neutron background produced by the stopping made little contribution to the bulk background.

TABLE I. The mean scattering energy calculated back from the range of the twice scattered protons and the detection thresholds used in the asymmetry measurement.

θ_2 c.m. (deg)	Mean scattering energy (MeV)	θ_2 c.m. (deg)	Mean scattering energy (MeV)	Detecting thresholds; minimum scattering energy (MeV)		
30L	210±2	30R	209±2	169	184	197
40L	214	40R	206	174	190	205
50L	212	50R	210	162	180	197
60L	212	60R	209	157	179	199
70L	215	70R	211	143	170	195
80L	215	80R	211	177	186	206
90L	215	90R	212	172	···	194
	Average: 213±1		Average: 210±1	Low	Intermediate	High

F. Facilities for Alignment of the Scattering Geometry

The polarimeter and the lead shield were mounted on a large turntable. The axis of rotation of the turntable was the vertical line going through the beam center at $T_2(D)$.

In order to set the second-scattering angle and to align the polarimeter axis in the effective center line of the twice-scattered beam, a goniometer, with its axis of rotation vertical, was placed at $T_2(D)$. The position of the goniometer axis could be varied by known amounts in the two directions s, and t, in the second-scattering plane, i.e., along and perpendicular to the incident beam (see Fig. 2). A plane mirror was attached on the goniometer in such a way that a scratch on its reflecting surface coincided with the rotation axis.

With this facility, one could mark a point in the scattering plane whose coordinates (s,t) could be read off. The origin of the (s,t) coordinate was conveniently chosen to be the effective beam center at $T_2(D)$ measured with the highest range threshold.

The mirror on the goniometer was used to set the axis of the polarimeter to any specified second-scattering angle θ_2 and to a scattering center (s,t) with help of an optical telescope (see Fig. 2) aligned normal to the mirror surface.

G. Electronics

The electronic circuitry for the asymmetry measurement consisted of conventional components. Two stages of coincidence circuits registered triple scattering events: the first stage registered the coincidences;

$$\mathrm{II}=(21,22);$$

$$\mathrm{III_aA}=(31a,32a); \qquad \mathrm{III_bA}=(31b,32b);$$

$$\mathrm{III_aB}=(31a,32a,33a); \qquad \mathrm{III_bB}=(31b,32b,33b).$$

The second stage detected the coincidences;

$$\mathrm{IV_aA}=(\mathrm{II},\mathrm{III_aA}); \qquad \mathrm{IV_bA}=(\mathrm{II},\mathrm{III_bA});$$

$$\mathrm{IV_aB}=(\mathrm{II},\mathrm{III_aB}); \qquad \mathrm{IV_bB}=(\mathrm{II},\mathrm{III_bB}).$$

The outputs of all the coincidence circuits were recorded simultaneously: those of the first stage gave a check on the performance of the circuitries and the counters.

Random counts in the IV rates were examined by introducing a delay of 50 nsec between the first and the second coincidence stage.

The resolving time of the coincidence circuitry was approximately 10 and 14 nsec for the first and the second stage, respectively.

Separate coincidence circuits were provided for the measurements of range curves and various beam profiles.

III. EXPERIMENTAL PROCEDURE

A. Range Curves and Range Requirements

At every angle of the second scattering, we obtained range curves of protons scattered by the hydrogen target. From those we calculated the mean scattering energy. The result is given in Table I. The mean scattering energy was higher for scattering to the left than scattering to the right. The shape of the range curve was also different for these two cases. The most sizable difference was found at $\theta_2=90°$ c.m., as shown in Fig. 3.

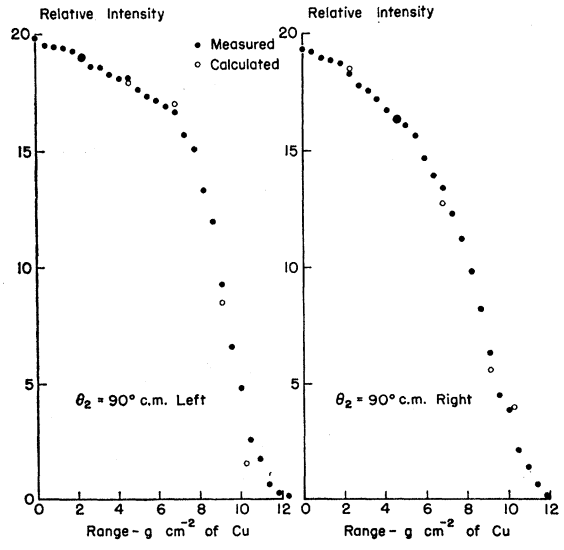

FIG. 3. Range curves of the twice scattered protons at $\theta_2=90°$ c.m. Normalization of the calculated points is made at 2.27 g cm^{-2} of copper on the "left" curve.

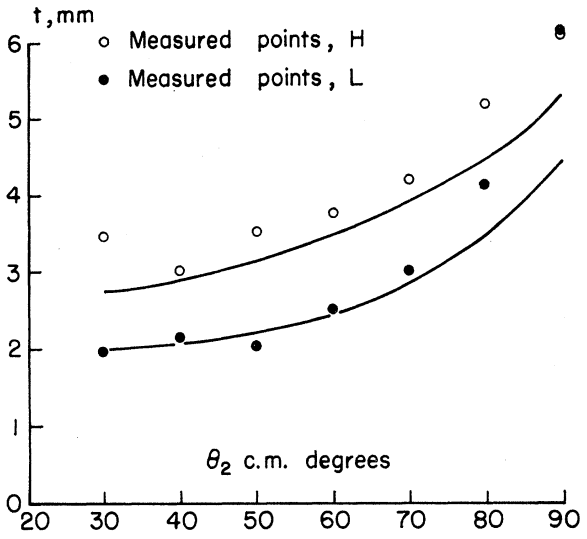

FIG. 4. The apparent transversal shift of the effective second scattering center. The upper and lower curves are the expected shifts calculated from the measured fringing field for the high and the low counting threshold, respectively. The origin of the "t" scale is chosen to be the centroid of the beam distribution measured with the high counting threshold. The points H and L are the measured values with the high and the low threshold.

The differences in range curves of left and right scattering can be explained by the characteristics of our polarized proton beam (II B and Fig. 1): The proton beam diverges with its virtual source at a point about 60 cm upstream from $T_2(D)$. There is a strong correlation between the mean energy and position at $P(D)$ which corresponds to an energy variation of 6 to 7 MeV for one degree of angular divergence from the center line of the beam, the rays which diverge to the left having smaller mean energies.

Assuming a point scattering center at $T_2(D)$ and taking into account the finite solid angle used in range measurement as well as nuclear absorption in absorbers, we can calculate what we should expect for left- and right-range curves for our proton beam scattering from a hydrogen target. Figure 3 shows the measured range curves of the twice-scattered protons at $\theta_2=90°$ c.m. together with the calculated points, which reproduce the observed difference quite well.

Proper range requirement in the asymmetry measurement is quite important, because excessive absorbers will introduce a large intensity variation over the third scatterer and thus produce a false asymmetry. To ensure this point we employed at least two or three different range requirements for each θ_2, so that we could examine how obtained asymmetries would depend on range thresholds. The highest range thresholds were set approximately on the knees of the range curves.

The data for two different range thresholds were collected simultaneously by using the III telescopes as double- and triple-coincidence telescopes with two sets of copper absorbers in between the counters. Then the absorbers were changed in such a way that the new range threshold for double coincidence was exactly the same as the old one for triple coincidence. In this fashion we obtained asymmetries for three different range requirements; the data for the intermediate range threshold were collected with both triple and double coincidences and therefore had better statistics than those for the other two range thresholds. The last column of Table I shows the range thresholds actually used in terms of the mean hydrogen-scattering energy: the low and high thresholds were 14 to 20 MeV above or below the intermediate threshold.

B. Alignment of the Polarimeter

Since the experiment is to measure the asymmetry of the third scattering, it is quite important to place the polarimeter in such a way that the average direction of the twice scattered beam is parallel to the axis of the polarimeter.

There are a few major effects which will shift the effective second-scattering center away from the previously obtained beam center at $T_2(D)$: Bending of the twice scattered beam due to the fringing field of the cyclotron gives an apparent shift transverse to the incident beam direction (in the t direction). Attenuation of incident protons in the hydrogen target and p-p scattering kinematics in the target of finite size will shift the center along the incident beam direction (in the s direction).

From the values of the vertical component of the fringe field measured along the average path of the twice-scattered protons, we calculated the apparent shift of the center for every θ_2. The shift turned out to be practically of the same amount for left and right scattering with the same θ_2. In Fig. 4 the expected shifts in the t direction are shown with two solid lines for the two range requirements. The shift along the s direction is somewhat harder to estimate. We estimated, however, that the upper limits of the shift due to attenuation and kinematics would be about 1.8 mm and 0.5 mm, respectively.

These estimated values were compared with shifts of the effective scattering center obtained experimentally as follows: We placed the geometrical center of the polarimeter slit at any desired second-scattering angle, then measured with the B telescope the horizontal profile of the beam accepted by the II telescope and the slit. The polarimeter tail was rotated around the vertical axis going through the center of the slit until the centroid of the profile came on the axis of rotation of the polarimeter. The profiles were measured with the absorbers which corresponded to the two extreme counting thresholds in asymmetry measurements.

This procedure contains an assumption that the geometrical center of the slit is the effective center of the beam distribution over T_3. Because of the kine-

TABLE II. Typical counting rates per minute at $\theta_2=80°$ c.m. The symbols for the different types of counts are defined in Sec. IIG of the text. (L) and (R) for III and IV rates indicate the third scattering to the left and to the right, respectively. III and IV are given for the average of the a and b telescope.

θ_2	T_2	T_3	II	III $A(L)$	III $B(L)$	IV A(L)	IV $B(L)$	III $A(R)$	III $B(R)$	IV $A(R)$	IV $B(R)$
80°L	Full	In	4.6×10^4	1.6×10^3	138	54	30	1.6×10^3	81	40	23
	Full	Out	4.6×10^4	1.5×10^3	125	12.0	2.3	1.4×10^3	55	7.3	2.2
	Empty	Out	1.5×10^4	1.3×10^3	90	1.5	0.5	1.3×10^3	50	1.2	0.5
	Empty	In	1.5×10^4	1.3×10^3	90	4.4	2.2	1.3×10^3	45	4.1	2.0
80°R	Full	In	4.3×10^4	1.3×10^3	76	39	20	1.3×10^3	78	39	18
	Full	Out	4.3×10^4	1.3×10^3	70	6.6	1.7	1.3×10^3	66	7.8	1.6
	Empty	Out	1.5×10^4	1.2×10^3	50	1.3	0.5	1.2×10^3	52	1.1	0.3
	Empty	In	1.5×10^4	1.2×10^3	71	5.1	2.1	1.2×10^3	61	4.3	1.6

matical energy change and cross-section variation in p-p scattering, this does not hold exactly. However, the false asymmetry due to these effects was negligibly small. The details of this point will be discussed in III E.

Since we expected the same amount of the shift along the t direction for left and right scattering with the same θ_2, we could locate the effective scattering center in terms of the (s,t) coordinates by obtaining the intercepting point of the aligned polarimeter axis in left and right scattering positions. Values of "t" thus obtained are included in Fig. 4. The measured values of "s" were (3 ± 1) mm and (1.5 ± 1) mm for all values of θ_2 for the high- and low-counting thresholds, respectively.

These results indicated that the limit of accuracy in the alignment was approximately ±1 mm at T_2, corresponding to ±3 min of arc in θ_3.

For asymmetry measurements the polarimeter was placed according to one of the measured alignments. We made no correction for small misalignment to the data which were taken with intermediate counting thresholds, since the correction would be at most 2 min. of arc in θ_3.

C. Asymmetry Measurement

The entire experiment was made in three separate runs. Asymmetries at 60° c.m. left and right were measured in all three runs, those at 30° c.m. in the last two runs. The rest of the data were collected in the last run.

For the asymmetry measurement the rates IV's were measured with all possible permutations of the following conditions: with different absorbers in the III telescopes, which corresponded to the counting thresholds listed in Table I; the hydrogen target cup full and empty; the polarimeter arm in its normal and inverted positions; the third target T_3 in and out (simultaneously the compensating absorbers out and in). The random coincidence rates were negligible at all angles.

In data-taking runs, an air-filled ionization chamber placed in front of the wedge magnet and intercepting the incoming polarized proton beam was used as a monitor.

One set of measurement at a chosen θ_2 was made as follows: With the target full, counts were collected on one side of the incident beam; then the turntable which carried the whole third-scattering apparatus was driven to the other side of the beam to collect target full counts at the same angle θ_2 on the other side. The empty target run followed in a similar fashion. In order to avoid effects due to drift of the electronics circuitry and fluctuation of the beam position, the polarimeter arm was turned over every ten minutes or so and the sign of θ_2 was switched every two hours. The alignment of the polarimeter axis was reproduced optically when it was necessary. The reproducibility was as good as the accuracy we obtained in our original determination of the correct alignment.

At each θ_2 the counts were accumulated in several sets of measurements until the over-all statistical error in asymmetry (for each range threshold setting) became comparable to the inherent error due to our limited accuracy in alignment.

Table II gives an example of counting rates in a set of measurements.

D. Calibration of Analyzing Power

To measure the analyzing power $e_c=P_1P_3$ of the polarimeter the polarized proton beam was slowed down with a lead degrader placed at $T_2(D)$. The geometrical center of the polarimeter slit was placed at the centroid of the degraded beam distribution measured at $P(D)$. The alignment of the polarimeter axis to the degraded beam was done in the manner similar to the case of hydrogen scattering. Thickness of degrader was adjusted so that the mean range of the degraded beam matched the average of the mean ranges of protons scattered to left and right with the corresponding θ_2. The matching of the ranges was accomplished with an accuracy of about ±0.4 g/cm^2 of copper by adjusting thickness of copper sheets attached to the main body of the degrader. Values of e_c for each θ_2 were obtained with exactly the same absorber settings in the III telescopes as used in hydrogen scattering.

e_c was measured with a statistical accuracy of ±0.012 to ±0.006. As the maximum alignment uncertainty for e_c measurement we chose ±0.008-±0.004

TABLE III. Some characteristics of the polarimeter.

θ_2 c.m.	e_c [a]	$-de_c/dR$ [b] (per g cm^{-2} of copper)	$\lvert de/d\theta_3 \rvert$ [c] (per min of arc)
30°	0.479±0.006	0.0031±0.0005	0.0025±0.0004
40°	0.415±0.006	0.0053±0.0009	0.0022±0.0004
50°	0.383±0.007	0.0079±0.0009	0.0020±0.0004
60°	0.324±0.007	0.010 ±0.001	0.0018±0.0004
70°	0.214±0.010	0.012 ±0.001	0.0016±0.0004
80°	0.156±0.011	0.014 ±0.001	0.0015±0.0005
90°	0.103±0.007	0.020 ±0.002	0.0013±0.0007

[a] The analyzing power of the polarimeter measured with a matched degrader for the lowest range threshold. The errors are statistical.
[b] The dependence of e_c on a small change in the mean range R of the protons on the analyzing target T_3.
[c] The sensitivity of e_c to a misalignment in θ_3.

in e_c for 30° c.m. through 90° c.m. These values were deduced from our limit of accuracy (±3 min of arc in θ_3) in the alignment which was discussed for the case of hydrogen scattering (see Table III).

Since, as shown in III A, the left and the right scattering from hydrogen gave slightly different mean ranges for the same θ_2, the final values of e_c were obtained by applying a small range correction to the measured values. This correction was determined by measuring e_c with degraders which were slightly thicker or thinner than the matched ones. The first three columns of Table III are the lists of the e_c's obtained with the matched degraders and the sensitivity of e's to a small change in the mean range of the protons incident on T_3. The amount of the range correction was not larger than (0.007±0.001) in e_c.

E. Spurious Asymmetry

There are several causes for possible spurious asymmetry in the measurement of the asymmetry in p-p scattering: (1) misalignment of the polarimeter axis in the scattering plane, (2) nonuniform beam intensity distribution over T_3, and (3) energy variation of the incident protons across T_3.

The amounts of these spurious asymmetries were estimated as follows: (1) The polarimeter in the calibration geometry for 30, 60, and 90° c.m. was misaligned by about ±0.5° and ±1° in θ_3 to obtain the change in e_c due to the misalignment. The sensitivity of asymmetry to misalignment ($de/d\theta_3$) thus obtained and interpolated to the other angles are listed in the last column of Table III. The measured ($de/d\theta_3$)'s indicate that the uncertainty in asymmetry with our alignment accuracy is ±0.008 to ±0.004 depending on the incident beam energy (2) and (3). Due to the p-p scattering kinematics and the angular distribution there are the variations of proton energy and intensity over the analyzing target T_2. The angular acceptance of the polarimeter was ±1.3° in the laboratory system, which gave the maximum amounts of energy and intensity variations of ±4.5 MeV and ±2.6%, respectively, at 90° c.m.

The nonuniformity of the intensity makes the effective beam center deviate from the geometrical center of the slit. The misalignment in terms of θ_3, however, was negligible due to the fact that we measured the beam profile at the position of the B telescope and aligned the polarimeter axis to coincide the effective center of the proton intensity distribution at this point. A simple calculation showed that the maximum expected intensity variation over T_3 of the twice-scattered protons gave a misalignment less than 2 min of arc in θ_3. Thus, it was justified within our alignment accuracy to take the geometrical center of the polarimeter slit as the approximate effective beam center.

The energy change over T_3 was not fully taken into account in our alignment procedure. A measurement was performed to obtain the typical amount of the spurious asymmetry introduced by this fact. A wedge-shaped thin absorber was placed in front of the polarimeter slit so as to get the expected maximum energy variation from the one edge of the slit to the other. The polarimeter was placed in the degraded beam corresponding to 90° c.m. The asymmetry was measured and compared with that obtained with a flat absorber whose thickness was equal to the mean thickness of the wedge absorber. The observed difference in asymmetry was 0.006±0.006; therefore, the correction for this was negligible.

IV. TREATMENT OF THE DATA AND THE RESULT

A. Outline of the Calculations

One can compute the depolarization parameter from the obtained data in two different ways: The one is to use Eqs. (3a) and (3b) with the knowledge of $P_2(\theta_2)$ and $P_2'(\theta_2)$ to obtain $D(\pm\theta_2)$, then to take their average as the final value $D(\theta_2)$. This way one can treat the p-p scattering to left and to right independently. The other way is to combine the data taken on both sides of the polarized beam and use the sum and the difference of Eqs. (3a) and (3b) and the expression for $P_2(\theta)$:

$$2D=(e_L/e_c)(1+P_iP_2)+(e_R/e_c)(1-P_iP_2), \quad (5)$$

$$2(P_2'/P_i)=(e_L/e_c)(1+P_iP_2)-(e_R/e_c)(1-P_iP_2), \quad (6)$$

$$P_2=[I(L)-I(R)]/[I(L)+I(R)], \quad (7)$$

where $I(L)$ and $I(R)$ are the sum of the net counting rates for the triple scattering to θ_2 left and right, respectively. The second method is, in general, a better approach for the amount of the data we obtained, since one can obtain P_2 and P_2' at the same time and can have a check of consistency of all the data. As far as the D parameter is concerned, however, both methods should give the identical result provided that P_2 used in one method is the same as the result in the other. Nevertheless, we employed the first method to compute the final result of the depolarization parameter, because

TABLE IV. The list of (e/e_c) in the scattering to left and to right for each range requirement.

θ_2 c.m.	Range[a] thresholds	$(e/e_c)\pm\Delta(e/e_c)$ L	$(e/e_c)\pm\Delta(e/e_c)$ R	$[(e/e_c)\pm\Delta(e/e_c)]_{av}$ L	$[(e/e_c)\pm\Delta(e/e_c)]_{av}$ R
30°	L	0.439±0.040	−0.204±0.044		
	I	0.435±0.040	−0.166±0.042		
	H	0.445±0.037	−0.206±0.040		
				0.438±0.023	−0.185±0.024
40°	L	0.440±0.040	−0.138±0.046		
	I	0.438±0.040	−0.142±0.043		
	H	0.440±0.042	−0.132±0.048		
				0.439±0.025	−0.138±0.026
50°	L	0.454±0.045	−0.156±0.049		
	I	0.455±0.023	−0.115±0.030		
	H	0.405±0.037	−0.076±0.045		
				0.444±0.015	−0.116±0.019
60°	L	0.505±0.046	−0.116±0.063		
	I	0.500±0.050	−0.145±0.057		
	H	0.454±0.046	−0.005±0.057		
				0.490±0.029	0.020±0.034
70°	L	0.541±0.070	−0.021±0.121		
	I	0.434±0.033	0.133±0.045		
	H	0.373±0.091	0.224±0.072		
				0.432±0.025	0.116±0.034
80°	L	0.379±0.135	0.251±0.108		
	I	0.536±0.056	0.205±0.065		
	H	0.506±0.090	0.161±0.141		
				0.489±0.041	0.205±0.045
90°	L	0.622±0.214	0.230±0.157		
	H	0.732±0.115	0.407±0.133		
				0.676±0.085	0.319±0.091

[a] H, I, and L correspond to the detecting thresholds listed in Table I.

the difference in the energy spectrum and the mean energy of the left and the right twice-scattered protons did not always allow us to use Eq. (7) to obtain the actual value of P_2; the right-hand side of Eq. (7) was calculated as a function of the range of the twice-scattered protons from the range curves measured at each θ_2 left and right. At all θ_2 this quantity remained constant within the statistical errors, if the range was not larger than the value which corresponded to the intermediate counting threshold imposed in the asymmetry measurement. Above the knee of the range curve, where the highest counting thresholds were set, it increases steeply and was determined largely by detailed shapes of the curves. Thus, to use the second method of analysis, we had to discard the data obtained with these highest range thresholds. In Sec. E we discuss P_1, P_2, and P_2' calculated by use of Eqs. (5), (6), and (7) from about three-quarters of the whole data for which we can use Eq. (7), in order to see the consistency of, at least, this part of the data.

B. Errors and Corrections for $e(\pm\theta_2)$ and $e_c(\pm\theta_2)$

The uncertainty in alignment of ±3 min of arc in θ_3 was combined with the statistical error in the squares, giving the total error in asymmetry $e(\pm\theta_2)$. The total error assigned to $e_c(\pm\theta_2)$ was the statistical combination of the alignment uncertainty, counting statistics, and the error in the range correction.

C. The Statistical Check of the Data

For each set of measurements (e/e_c) was computed separately for the a and b telescope. The mean deviation between (e/e_c) obtained with the two telescopes was compared with the statistical error. The deviations at all angles were consistent with the statistically expected differences.

In Table IV (e/e_c)'s, which were calculated from the combined results with the both telescopes, were given for different detection thresholds. Although these at 60 and 70°R vary somewhat more than what one would expect from the total errors, there is no systematic dependence of (e/e_c) on the range threshold. Therefore (e/e_c)'s with different range requirements were averaged to obtain the final values of (e/e_c). These are also given in Table IV.

D. $D(\theta_2)$

The depolarization parameter was calculated for scattering to left and to right from the final values of (e/e_c). For the values of P_2 and P_2', assuming the time reversal invariance,[13] we used the result of the asymmetry measurement in p-p scattering (see Table VI) which was made recently by Warner and Tinlot.[14]

[13] R. T. N. Phillips, Nuovo cimento **8**, 265 (1958); A. Abashian and E. M. Hafner, Phys. Rev. Letters **1**, 255 (1958); P. Hillman, A. Johansson, and G. Tibell, Phys. Rev. **110**, 1218 (1958); C. F. Hwang, T. R. Ophel, E. H. Thorndike, and R. Wilson, *ibid.* **119**, 352 (1960).

[14] J. H. Tinlot and R. Warner, Phys. Rev. **124**, 890 (1961).

TABLE V. The final result of the depolarization parameter $D(\theta_2)$ in p-p scattering at 213 MeV.

θ_2 c.m.	$D(\pm\theta_2)$ [a] Left	Right	Averaged	$D(\theta_2)$ [b] Final value
30°	0.210±0.035	0.215±0.031	0.213±0.024	0.200±0.016
40°	0.206±0.028	0.258±0.031	0.232±0.026	0.232±0.026
50°	0.224±0.019	0.255±0.028	0.240±0.018	0.240±0.018
60°	0.325±0.035	0.286±0.048	0.306±0.032	0.319±0.021
70°	0.311±0.038	0.283±0.034	0.297±0.030	0.297±0.030
80°	0.427±0.046	0.290±0.044	0.36 ±0.07[c]	0.36 ±0.07[c]
90°	0.675±0.083	0.317±0.090	0.50 ±0.18[c]	0.50 ±0.18[c]

[a] The result of the final run.
[b] The previously obtained 30° and 60° results[9] are included.
[c] See the text, Sec. IV D, about the errors.

0.89±0.02 was used for P_i, the initial value of the beam polarization.

The first three columns of Table V give $D(\pm\theta_2)$. The two values of the depolarization parameter at θ_{2L} and θ_{2R} are in fair agreement up to 70° c.m. At 80° c.m. and 90° c.m., however, the results differ by three to four standard deviations. Although this fact, especially the discrepancy at 90°, was realized during the measurement, we found no instrumental mistake which might be the cause. Since the results at these angles seem to indicate some possible unknown error, we take some reservations for the results at 80° c.m. and 90° c.m. by quoting the average of the left and the right values with somewhat arbitrarily assigned errors so that the limits of the errors reach to the left or the right values.

As the values of the depolarization parameter at 30 through 70° c.m. the arithmetic average of $D(\pm\theta_2)$ was taken because the absolute errors in (e_L/e_c) and (e_R/e_c) were nearly equal at all the angles. The errors for the averaged values were calculated in such a way that the error due to the term P_2'/P_i, which was canceled out by averaging the left and the right results, was not included. The final values are listed in the fifth column of Table V.

E. Consistency of the Data and 90° Result

Equations (5), (6), and (7) were used for all the asymmetry data except those with the highest range thresholds in order to see the consistency of the data. In Table VI thus calculated P_2, P_2', and D are listed with P_2 obtained by Tinlot and Warner[14] and also P_2 calculated from the range curves of the twice scattered protons in this experiment. The values of D appear to be insensitive to the omission of part of the data. The agreement between P_2 and P_2' at 80° c.m. is a somewhat fortuitous result of discarding a part of the data. At 90° c.m. P_2' comes out too high, indicating the discrepancy which appeared as the disagreement between $D(+\theta_2)$ and $D(-\theta_2)$ in the previous section.

The amount and the nature of the inconsistency at 90° c.m. can be shown in the following two ways, if one would attribute it entirely to a misalignment in θ_3; in one case one would require about 20 min of arc of misalignment in θ_3 in both left and right scattering. This misalignment must be the one along the s scale and must amount to about 8 mm to explain the inconsistency. In the other case about 40 min of arc misalignment in θ_3 would be necessary, in either the left or the right scattering, and this would correspond to the second scattering displaced by about 8 mm in both t and s scale. Thus, it is certainly impossible to explain the trouble only by θ_3 misalignment.

As the conclusion of the consistency check of the data, we regard the result at 90° c.m., which obviously includes unknown experimental error(s), as preliminary. Although the data at 80° c.m. may indicate the same type of inconsistency, it is much less pronounced and can well be considered as a large statistical fluctuation. At all the other angles the data are consistent as one expects from the agreement between D obtained in the left and right scattering.

V. DISCUSSION OF THE RESULT

A. Presently Available Experimental Data

There has been a substantial improvement in both the amount and the accuracy of the available experimental data on p-p interaction at 213 MeV since the results of the R and A measurements[3] were reported.

The unpolarized cross section $(d\sigma/d\Omega)$ and the asymmetry (P_2), for which we had the data only from a few old measurements at a slightly different interaction energy, e.g., 240 MeV for $d\sigma/d\Omega$, have been remeasured recently[5,14] with higher accuracy and at the correct energy. At present, in addition to these re-

TABLE VI. The consistency check of the data obtained with the intermediate and low range requirements.

θ_2 c.m. (deg)	$P_2(\theta_2)$ Tinlot-Warner[a]	Range curves[b]	D measurement[c]	$P_2'(\theta_2)$	$D(\theta_2)$
30	0.312±0.009	0.286±0.008	0.278±0.008	0.308±0.015	0.214±0.029
40	0.319±0.011	0.310±0.003	0.322±0.008	0.301±0.015	0.244±0.032
50	0.303±0.010	0.310±0.003	0.307±0.008	0.307±0.016	0.251±0.021
60	0.240±0.009	0.267±0.011	0.273±0.009	0.280±0.016	0.329±0.039
70	0.163±0.008	0.209±0.016	0.173±0.009	0.195±0.030	0.314±0.035
80	0.084±0.007	0.100±0.007	0.076±0.008	0.115±0.048	0.377±0.036
90	−0.001±0.007	0.023±0.010	0.000±0.007	0.173±0.080	0.426±0.090

[a] Asymmetry in p-p scattering measured by Tinlot and Warner (reference 14).
[b] Asymmetry deduced from the range curves of the twice-scattered protons in this experiment.
[c] Asymmetry obtained from the triple-scattering rates in this experiment.

TABLE VII. The unique phase shift sets[a] for p-p interaction at 213 MeV.

	g^2	$^1S_0$	$^1D_2$	$^3P_0$	$^3P_1$	$^3P_2$	e_2	$^3F_2$	$^3F_3$	$^3F_4$	χ^2	(Expected χ^2)
Solution b by McGregor *et al.*[b]	14[b]±2	5.13	6.78	−1.29	−22.07	15.94	−2.87	0.86	−2.44	1.72	48.5	(29)
Solution b by Signell[c]	14.4[c]±1.4	5.09±0.46	6.85±0.25	−1.58±0.53	−22.40±0.60	15.98±0.23	−3.01±0.19	1.00±0.40	−2.53±0.22	1.80±0.30	48.4	(29)
Hamada potential[d]		4.5	9.3	−2.8	−20.2	17.6	−2.4	1.1	−2.8	1.5	...	...
YLAM solution[e]		5.7 ±1.6	7.5 ±0.8	−1.2 ±3.7	−20.6 ±1.0	16.2 ±0.9	−2.6 ±0.5	0.6 ±0.3	−3.2 ±0.3	0.7 ±0.4	...	...

[a] Phase shifts are nuclear bar phase shifts (see reference 7) in degrees.
[b] Reference 17. The phase shifts and g^2 value are the results of their analysis in which the nine lowest phase shifts and the normalization factor for the absolute p-p cross section were searched on for several different values of g^2.
[c] Reference 18. These are the results of his analysis with nine phase parameters and g^2 values searched on. The errors on the phase shifts are the diagonal elements of the error matrix.
[d] Reference 21.
[e] Reference 23.

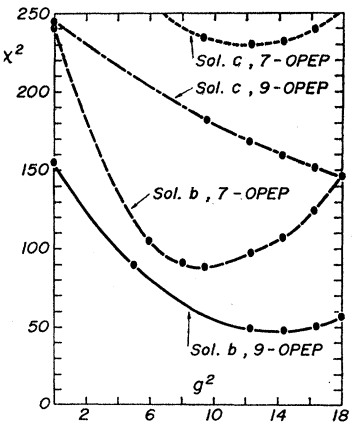

FIG. 5. g^2 dependence of χ^2 for solutions b and c (reference 17). The points are for the phase shift solutions from the modified phase-shift analysis using nine or seven lowest phases as free parameters, the higher waves being given by OPEP, one pion exchange contribution. The expected χ^2 is 30 for the nine parameter search.

measured results, we have available, the results for R A, and D described in this article at seven angles from 30 to 90° c.m. and the preliminary result for[15] R' at 30, 40, 50, and 60° c.m.

B. Analysis

As briefly described in the introduction of this paper, the modified phase-shift analysis[7] has been applied to the data at 213 MeV to search for a unique phase shift solution at this energy. The two earlier searches[6,9] gave quite encouraging results despite the fact that they were based on the data which were not a complete set of experiments[16] and were preliminary and crude in comparison with the presently available data.

Very recently, new phase-shift searches have been in progress at Livermore[17] and also at Pennsylvania State University[18] using these presently available data listed above. Only two phase-shift sets have been found, whose χ^2 are reasonably close to the expected value. Those are the solutions of type b and c as labeled by MacGregor *et al.*[6] Figure 5 summarizes the results obtained by the Livermore group: Their nine parameter search for a type b solution with several different values of the pion-nucleon coupling constant g^2 gives a minimum value for χ^2 of 49. The best g^2 value is 14±2. The expected χ^2 for a nine parameter search is 30.

The other group obtained an identical result from a phase-shift analysis with nine phases and g^2 as parameters.

The χ^2 value for solution c is approximately 150 at $g^2=14.4$. If we consider the g^2 dependence of the χ^2 for the two solutions (Fig. 5) and also the fact that the solution b is the phase-shift set which goes over smoothly

[15] F. Lobkowicz and K. Gotow (private communication).
[16] L. Puzikov, R. Ryndin, and J. Smorodinskii, J. Exptl. Theoret. Phys. (U.S.S.R.) **32**, 592 (1957) [translation: Soviet Phys.—JETP **5**, 489 (1957)]; L. G. Zastavenko, R. Ryndin, and Chou Guan-chao, J. Exptl. Theoret. Phys. (U.S.S.R.) **34**, 526 (1958) [translation: Soviet Phys.—JETP **7**, 363 (1958)]; Nuclear Phys. **6**, 669 (1958).
[17] M. H. MacGregor, M. J. Moravcsik, P. H. Noyes, and P. H. Stapp (private communication).
[18] P. Signell (private communication).

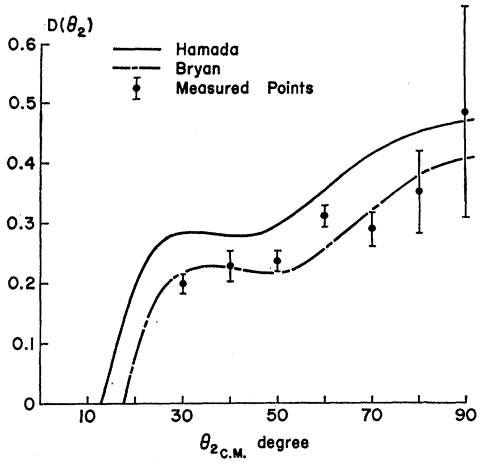

FIG. 6. Comparison of the experimental result with the predictions by the semiphenomenological potentials of Hamada (see reference 21) and of Bryan (see reference 19).

to the most preferred solutions at other energies, we can say that a unique set of phase shifts at 213 MeV is now established. The unique sets obtained by Moravcsik *et al.* and by Signell are shown in Table VII.

The attempt to interpret the p-p experimental data over the whole energy range has been pushed forward by further refinements of semiphenomonological potentials[19–21] and also by energy-dependent phase shift analysis.[22,23] We merely state here that the phase shifts obtained from the potentials in references 19, 20, and 21 and also the best energy-dependent phase shifts[22,23] are of type b. For comparison we list the typical sets in Table VII. Figure 6 compares our results for the D-parameter with the predictions made from the potentials of Bryan[19] and of Hamada.[20]

Despite the rather convincing evidence for the uniqueness of the solution b, it is still not quite a statistically acceptable solution.

In Table VIII the breakdowns of the χ^2 sums are given for solutions b and c.[24] If we restrict ourselves to the depolarization parameter alone, then solution b gives a far better fit to the data than solution c, the χ^2 of

TABLE VIII. Breakdown of χ^2 sum for solutions b and c.[a]

Solution b: $g^2=14.4$;			χ^2 sum = 58;		Expected $\chi^2=30$	
θ_2 c.m.	$d\sigma/d\Omega$	P_2	D	R	R'	A
30°	2.04	1.37	0.75	0.45	0.74	3.15
40	0.29	0.66	0.07	0.18	1.68	0.00
50	0.53	0.04	0.05	0.04	5.21	0.29
60	1.11	0.04	4.66	0.82	3.01	0.01
70	0.01	2.39	0.00	0.00	···	0.32
80	0.66	0.03	0.66	0.23	···	10.61
90	0.13	0.02	0.86	0.87	···	13.08
Partial sum	4.8	5.5	7.1	2.6	10.6	27.5
Solution c: $g^2=14.4$;			χ^2 sum = 176;		Expected $\chi^2=30$	
30°	0.02	5.80	2.62	0.80	4.17	5.66
40	0.00	1.34	0.32	0.01	0.31	2.21
50	0.39	1.20	1.46	0.00	3.44	8.08
60	0.72	1.35	0.15	0.02	2.65	2.85
70	0.00	1.09	12.46	1.38	···	1.41
80	0.19	2.87	4.73	0.73	···	40.36
90	0.07	0.02	0.11	7.26	···	57.23
Partial sum	1.4	13.7	21.9	10.2	10.6	117.8

[a] See footnote 24.

which can occur with a probability of less than 0.1%. One has to keep in mind, however, that the errors for 80 and 90° c.m. have been given rather arbitrarily so that those two points do not contribute much to the χ^2 sum nor to the experimental information. We notice that at 80 and 90° c.m. the values of the A parameter give excessively large χ^2 contributions to both solutions, which indicate some doubt about the accuracy of either the measured values or the assigned errors. In fact, if we omit these two points, the χ^2 for the solution b with $g^2=14.4$ becomes statistically acceptable; 34 for the expected 28, while that for the solution c with $g^2=14.4$ is 78. Therefore, we intend to remeasure A as well as D at these two angles in the near future.

C. Further Experimental Study

It is probable that the remeasurement of the D and A parameters at 80 and 90° c.m. will change the χ^2 sums so that we may be able to be definitive on the unique phase-shift solution at 213 MeV. We hope that the remeasurement of these large-angle points also serves as the means to assess the amount of possible systematic error which otherwise is unknown.

ACKNOWLEDGMENTS

We wish to thank Dr. P. H. Noyes, Dr. M. J. Moravcsik, Dr. M. H. MacGregor, and Dr. H. P. Stapp, and also Dr. P. Signell, for sending us the results of their analysis prior to publication. We also thank Professor J. H. Tinlot for many valuable discussions.

[19] R. A. Bryan, Nuovo cimento **16**, 895 (1960).
[20] D. P. Saylor, R. A. Bryan, and R. E. Marshak, Phys. Rev. Letters **5**, 266 (1960).
[21] T. Hamada, Progr. Theoret. Phys. (Kyoto) **24**, 220 (1960); *ibid.* **24**, 1033 (1960).
[22] H. P. Stapp, H. P. Noyes, and M. J. Moravcsik (private communication).
[23] G. Breit, M. H. Hull, Jr., K. E. Lassila, and K. D. Pyatt, Jr., Phys. Rev. **120**, 2227 (1960).
[24] The χ^2 used in Table VIII are not for the best-fit solutions of type b and c, but for the "nearly best" solutions. Hence, the χ^2 in the table are slightly higher than those given for the best-fit solutions. The essential features, however, remain unchanged for the best solutions of type b and c.